Journal of Current Science and Technology, April - June 2025 Vol. 15 No. 2, Article 100

ISSN 2630-0656 (Online)

Cite this article: Miftahurrohmah, B., Cholilie, I. A., Wijaya, S. U., Atmaja, F., Bariyah, T., & Wulandari, C. (2025). Future growing seasons: bias correction with svr and qdm for indonesian temperature projection under RCP 2.6 and RCP 8.5. *Journal of Current Science and Technology*, *15*(2), Article 100. https://doi.org/10.59796/jcst.V15N2.2025.100

Journal of Current Science and Technology

Journal homepage: https://jcst.rsu.ac.th

Future Growing Seasons: Bias Correction with SVR and QDM for Indonesian Temperature Projection under RCP 2.6 and RCP 8.5

Brina Miftahurrohmah[1,*], Irvan Adhin Cholilie[2], Sekarsari Utami Wijaya[3], Felix Atmaja[1], Taufiqotul Bariyah[4], and Catur Wulandari[1,5]

[1]Department of Information Systems, Universitas Internasional Semen Indonesia, Gresik, Indonesia
[2]Department of Agroindustrial Technology, Universitas Internasional Semen Indonesia, Gresik, Indonesia
[3]Department of Logistics engineering, Universitas Internasional Semen Indonesia, Gresik, Indonesia
[4]Department of Informatics, Universitas Internasional Semen Indonesia, Gresik, Indonesia
[5]Interfaculty Center for Teacher Training, Educational Research and Further Training of Leiden University, Leiden, Netherland

*Corresponding author; E-mail: brina.miftahurrohmah@uisi.ac.id

Received 15 July, 2024; Revised 30 September 2024; Accepted 2 December 2024; Published online 25 March 2025

Abstract

Human activities have significantly contributed to greenhouse gas (GHG) emissions, escalating global temperatures and exacerbating extreme weather events, which pose serious agricultural threats by disrupting crop growth. Climate researchers employ Representative Concentration Pathways (RCPs) to forecast future GHG scenarios. Downscaling techniques have improved predictions of Growing Season Lengths (GSL) predictions and mean temperatures (T_{mean}), both of which are crucial for agricultural planning. This study evaluated Support Vector Regression (SVR) and Quantile Delta Mapping (QDM) for projecting T_{mean} and its impact on GSL under RCP 2.6 and RCP 8.5. Bias correction was applied to historical T_{mean} data using both methods, based on ERA5 data. SVR showed a lower Root Mean Square Error (RMSE) (0.6 vs 1.1) and a slightly higher correlation (0.6 vs. 0.5) than QDM. However, QDM was chosen for T_{mean} projection due to its superior data homogeneity and better alignment of standard deviation with observed values. Projections indicated a significant T_{mean} increase after 2026 under both RCPs, with T_{mean} under RCP 8.5 expected to exceed 30°C between 2050 and 2100, necessitating heat-resistant crop varieties. Greater increases in GSL under RCP 2.6 underscored the need for effective mitigation strategies. This study emphasizes adaptive farming practices and recommends integrating quantile-based and machine learning methods into future climate projections to enhance agricultural resilience.

Keywords**:** *bias correction; SVR; QDM; mean temperature; GSL; RCP 2.6; RCP 8.5.*

1. Introduction

Greenhouse gases (GHGs) and climate change are complex research topics and have been the focus of scientific studies for the past few decades. Anthropogenic activities, such as fossil fuel combustion, deforestation, and industrial processes, have significantly increased atmospheric GHG concentrations since the Industrial Revolution (Largeau et al., 2024). This phenomenon leads to rising global temperatures and climate change, resulting in extreme weather events such as higher air temperature, intensified tropical cyclones, floods, droughts, and other extreme events (Petchchedchoo et al., 2024; Khairulbahri, 2022). The impacts of these extreme climate changes can be severe to the agricultural sector (Cech et al., 2022; Liu et al., 2022). Temperature, as a climate variable, significantly influences food crop productivity (Qi et al., 2022). Extreme temperature conditions can physically and chemically affect crop growth and quality (Fernie et al.,

2022). Extreme and fluctuating temperature conditions can also impact the development of weeds and herbicide efficacy in managing weed populations (Kumar et al., 2023). This can have a direct impact on crop productivity, including food crops (Kumari et al., 2022; Qi et al., 2022; Villa-Falfán et al., 2023; Zare et al., 2023). Climate change affects crop species differently, creating barriers to sustainable crop production, depending on the climate in each location (Kumari et al., 2022; Montero-martínez, & Andrade-velázquez, 2022; Villa-Falfán et al., 2023). In addition to negative impacts, temperature can also positively impact agricultural productivity (Gouveia et al., 2023). Therefore, climate projections, especially temperature, must be conducted for the near future to predict and schedule agricultural crop potential (Hinze et al., 2023).

Modeling scenarios for predicting future climate based on GHG atmospheric concentrations and emissions, air pollution, and land use have been developed. Such climate modeling scenarios are Representative Concentration Pathways (RCPs) used to assess the costs associated with emissions reductions consistent with a given concentration pathway. RCPs refer to the concentration pathways utilized in the IPCC AR5. The defining characteristic of the pathway is its radiative forcing in the late 21st century. In this context, the radiative forcing denotes the additional heat trapped in the lower atmosphere due to increased GHG, measured in Watts per square meter (W/m^2) (Jubb et al., 2013). The four RCPs represent different greenhouse gas emission levels: RCP 2.6 (low), RCP 4.5 and RCP 6.0 (medium), and RCP 8.5 (high) (National Climate Change Adaptation Research Facility, 2017; IPCC, 2015). In this study, the scenarios used are RCP 2.6 and RCP 8.5 to assess the impact of GHG emissions on future agricultural productivity and food quality. The U.S. Department of Agriculture applied both scenarios to assess food systems and food security in the context of climate change (Brown et al., 2015). Hinze et al., (2023) also successfully projected the climate regarding changes in vegetation potential with the RCP 8.5 future model.

As a global framework for modeling climate change, RCP scenarios often have a coarse resolution and inaccurate representation of local conditions. Therefore, a downscaling process is required to generate data with finer resolution and accuracy. This process enables a more comprehensive understanding of climate change on a local or regional scale. However, downscaling results are also susceptible to biases during the data transformation. To overcome this, bias correction methods are needed to reduce errors. A study showed that applying bias correction methods to RCP 2.6, RCP 4.5, and RCP 8.5 scenarios positively impacted daily precipitation and temperature and improved model performance in most observed cases and scenarios (Tan et al., 2020). The Quantile Delta Method (QDM) has proven to be one of the effective approaches in correcting the bias of downscaling results. Earlier research indicates that QDM typically achieves stronger correlations and lower mean square errors than conventional bias correction methods when matching downscaled results with observations (Fauzi et al., 2020; Kuswanto et al., 2022; Rajulapati, & Papalexiou, 2023; Xavier et al., 2022). In this context, our research also implements the Support Vector Regression (SVR) method as an alternative in the bias correction process. As one of the robust algorithms for handling non-linearity cases in data, SVR showed satisfactory performance in improving the downscaling results of temperature extremes in the Seoul city area, South Korea (Cho et al., 2020).

The importance of using observational data in the downscaling and bias correction process cannot be ignored. Observation data is the dependent variable, while RCP scenario data is the independent variable. In this study, we use observational data from the ERA5 reanalysis. ERA5 is superior to other global reanalysis, especially in predicting low wind speeds over the UK (Potisomporn et al., 2023). Research findings show high consistency between ERA5 trends and observations, suggesting that they are reliable surrogates for observational data (Yilmaz, 2023). While ERA5 offers valuable climate data for areas lacking gauges, it is advisable to apply bias correction before utilizing it, particularly in tropical regions (Tan et al., 2023). In addition, the accuracy of ERA5 has also been shown to be higher than that of MERRA-2 (Huang et al., 2023). Therefore, a thorough understanding of the significance and reliability of observational data and the selection of appropriate bias correction techniques is essential to ensure the precision and reliability of downscaling outcomes, particularly in local or regional climate change studies.

Growing Season Length (GSL) is a key ecological factor influencing vegetation productivity (Arslantaş, & Yeşilırmak, 2020; Barnard et al., 2018; Park et al., 2016; Wang et al., 2020; Zhou, 2020). GSL is considered crucial for enhancing crop productivity. A study was conducted to verify this hypothesis (Chen et al., 2016). Various studies in different countries have involved the GSL index in improving crop productivity (Calinger, & Curtis, 2023; Hudson et al., 2022; Ngongondo et al., 2014). GSL can be an

important indicator in determining the timing of crop planting, maintenance, and harvesting. The optimal length of the growing season can increase agricultural yields and crop productivity. Precise GSL data enables farmers to schedule planting and harvesting effectively, optimize resource use, such as water and fertilizer, and minimize crop failure risks caused by severe weather conditions. Government and relevant agencies can use GSL to plan agricultural activities, formulate policies, and manage natural resources sustainably. GSL information can also assist in mitigating the risk of agricultural disasters such as droughts or floods. GSL is pivotal in comprehending crop growth dynamics, identifying influential regional climate patterns, and predicting how climate change will affect agriculture in the future.

Mean temperature (T_{mean}) data is essential for obtaining Growing Season Length (GSL) information. In addition to being a key variable for calculating GSL, T_{mean} is also an important agrometeorological variable (Amien & Runtunuwu, 2009; Brown et al., 2015; Chancellor et al., 2021). Therefore, this study applied downscaling and bias correction to historical GCM T_{mean} data, comparing the Quantile Delta Mapping (QDM) and Support Vector Regression (SVR) methods to identify the most accurate approach for future T_{mean} prediction. The optimal method will then be used to project future T_{mean} under the RCP 2.6 and RCP 8.5 scenarios. Finally, the anomalies and differences in T_{mean} and GSL between these scenarios will be analyzed to assess future climate conditions.

2. Objectives

This research aims to compare the effectiveness of the SVR and QDM methods in correcting bias in mean temperature (T_{mean}). Evaluation criteria included RMSE, correlation, and standard deviation to assess each method's performance in maintaining data consistency. Additionally, the study aimed to forecast future T_{mean} and GSL under the RCP 2.6 and RCP 8.5 scenarios for Indonesia. Based on historical data and climate projections, the study analyzed fluctuations in T_{mean} and GSL, emphasizing how climate change impacts agricultural methods and food security throughout Indonesia. The study aims to provide insights into climate dynamics and support adaptation strategies for future food security.

3. Materials and Methods

3.1 Data Collection

This study uses daily data from the Global Climate Model (GCM), including historical records, RCP 2.6, and RCP 8.5 scenarios, specifically focusing on temperature variables derived from the BNU-ESM model. These data were obtained from the DKRZ website, with historical data from 1950 to 2005, and RCP data covering the period from 2006 to 2100. The BNU-ESM model, developed by Beijing Normal University, has a resolution of 2.8° × 2.8°. The historical dataset from 1950 to 2005 spans 20,453 days, with 152 location points per day, comprising 19 longitudes and eight latitudes, leading to a total of 3,104,488 data points. Meanwhile, the RCP data, consisting of RCP 2.6 and RCP 8.5, covers the period from 2006 to 2100 for 34,697 days, with the same number of location points, resulting in a total of 4,055,632 data. ERA5, developed by ECMWF as the latest generation of atmospheric reanalysis, provides comprehensive global climate data from 1950 to 2022. On the other hand, the ERA5 data from 1950 to 2022 covers 26,662 days, with 12,512 location points (variables) per day, consisting of 184 longitudes and 68 latitudes, resulting in a total of 333,592,544 data.

3.2 Data Historical Downscaling

Data downscaling was performed using historical and reanalysis data from the same period, applying "Climate Imprints" to each variable. These data were accessible at https://cera-www.dkrz.de (GCM BNU-ESM) and https://cds.climate.copernicus.eu/ (ERA5 Reanalysis). Downscaling techniques improve the resolution of larger climate data to a smaller resolution, making it more detailed and relevant for local or regional studies. Climate Imprints, developed by Hunter and Meentemeyer (2005), is available in the "ClimDown" package in R. This step produces historical data with a smaller resolution, corresponding to the resolution of the ERA5 reanalysis. Thus, the number of location points for BNU-ESM data, historical scenarios and RCP, becomes 12,512 location points (variables) per day, consisting of 184 longitudes and 68 latitudes. Thus, the number of location points for historical and RCP's scenarios becomes 12,512 location points (variables) per day, consisting of 184 longitudes and 68 latitudes.

3.3 Bias Correction of Historical Data with QDM and SVR

The downscaled data was then bias-corrected using two methods: QDM and SVR. QDM adjusts the quantile distribution of the data to the reference, while SVR improves the prediction with a more accurate

regression model. The SVR model used default parameters from the scikit-learn library to minimize computational burden due to the large dataset. The kernel function is the radial basis function (RBF) because it is generally better at handling non-linear datasets. Both approaches were examined to identify the most efficient method for minimizing inaccuracies and discrepancies in the data. For training the SVR model, the number of data points used is 255,907,936 (corresponding to 20,453 days from 1950 to 2005 and 12,512 location points) for each type of data: historical data serving as independent variables and ERA5 data as dependent variables. The training process was conducted separately for each variable and location. The results from this stage helped select the most suitable method to produce more accurate data for further analysis.

3.4 Evaluation of Method Performance

The next step involved evaluating the best method using Taylor diagrams, which incorporating three key metrics: Standard Deviation (*SD*), correlation coefficient (*r*), and Root Mean Square Error (*RMSE*). Taylor diagrams are a useful visual tool to compare the performance of different methods or models in predicting or improving data. The formulas of *SD, r,* and *RMSE* are as follows:

$$SD=\frac{SD_b}{SD_o}=\frac{\sqrt{\frac{\sum_{i=1}^{n}(b_i-\bar{b})^2}{n}}}{\sqrt{\frac{\sum_{i=1}^{n}(o_i-\bar{o})^2}{n}}} \quad (1)$$

$$RMSE=\sqrt{\frac{\sum_{i=1}^{n}(b_i-o_i)^2}{n}} \quad (2)$$

$$r=\frac{\sum_{i=1}^{n}(b_i-\bar{b})\,(o_i-\bar{o})}{\sqrt{\sum_{i=1}^{n}(b_i-\bar{b})^2\sum_{i=1}^{n}(o_i-\bar{o})^2}} \quad (3)$$

where *n* represents the quantity of data points, *b* denotes the output from the bias correction and *o* refers to the ERA5 data (observational data). $\bar{b}$ and $\bar{o}$ are the averages of the bias-corrected output and observational data. The criteria for selecting the best method are as follows. Standard Deviation (SD) measures the data spread from the mean value, with a normalized range from 0 to 1 by min max scaler feature (0,1) methods with Scikit-Learn Python. SD_{norm}, SD normalized, can be calculated using $SD_{norm}=\frac{(SD-\min(SD))}{(\max(SD)-\min(SD))}$ where max (SD) is 0 and min (SD) is 1. Results closer to 1 indicate a distribution closer to the reference distribution, suggesting better accuracy. The use of normalized standard deviation in this study ensures a uniform scale in calculations, facilitating easier comparisons between predictive models. Using normalized values also minimizes the impact of extreme data points that may exhibit significant variability in distribution. While it is acknowledged that employing actual standard deviation could provide a more comprehensive overview, the authors are considering incorporating this approach in a revised study version. Root Mean Square Error (RMSE) quantifies the discrepancy between predicted and reference values, where a lower RMSE signifies more accurate estimations by the model or method. The Correlation Coefficient (*r*) evaluates the linear alignment between predicted and reference values on a scale from 0 to 1. A stronger correlation, approaching 1, indicates more precise bias correction results, showcasing the method's effectiveness.

3.5 Downscaling and Bias Correction of RCP 2.6 and RCP 8.5

Downscaling and bias correction of RCP 2.6 and RCP 8.5 data were done using the best method obtained. The next step in this research is to perform downscaling and bias correction on RCP 2.6 and RCP 8.5 data. Downscaling uses the Climate Imprint method to increase the resolution of RCP 2.6 and RCP 8.5 data to the matching grid resolution as ERA5, the observation data, to make climate projections more accurate. The downscaling results were then bias-corrected using the best-evaluated method to reduce systematic errors and produce more reliable climate data.

3.6 Calculating the Growing Season Length (GSL)

The Growing Season Length (GSL) is determined by calculating the number of days between two key periods within a calendar year. In the Northern Hemisphere (1 January to 31 December), it is the number of days between the first period of at least six consecutive days with a daily T_{mean} above 5°C and the first period after 1 July with at least six consecutive days with T_{mean} below 5°C. In the Southern Hemisphere (1 July to 30 June), it is the number of days between the first period of at least six consecutive days with T_{mean} above 5°C and the first period after 1 January with at least six consecutive days with T_{mean} below 5°C. The GSL is calculated using T_{mean} from two climate scenarios, RCP 2.6 and RCP 8.5, using R software with the library climdex.pcic.

3.7 Performing the Wilcoxon test

The Wilcoxon rank sum test was used in this study to assess differences in daily T_{mean} between RCP 2.6 and RCP 8.5 scenarios, as well as between each scenario and historical data. This non-parametric test was chosen due to potential deviations from normal distribution assumptions. A significance level (α) of 0.05 is applied, where a P-value less than α provides evidence to reject the null hypothesis, indicating significant differences between the compared conditions. This approach helps ascertain variations in GSL between scenarios RCP 2.6 and RCP 8.5, and between these scenarios and historical data, contributing to a comprehensive analysis of climate change impacts. The Wilcoxon sign rank test formula is shown in equations (4) and (5).

$$W=R-\frac{1}{2}n_2(n_2+1) \quad (4)$$

$$Z=\frac{W-\frac{n_1n_2}{2}}{\sqrt{n_1n_2\frac{(n_1+n_2+1)}{12}}} \quad (5)$$

The sum of the ranks of observations from population II (n_2) is denoted as R, where the values in population II (n_2) are greater than those in population I (n_1).

4. Results

4.1 Performance Comparison Between QDM and SVR methods

Figure 1(a) presents the comparative outcomes of bias correction methods, specifically utilizing SVR and QDM. The projection results showed that the correlation between projection and SVR (0.6) was higher than with QDM (0.55), indicating a stronger correlation with observations. In addition, the error rate measured using RMSE was also smaller for SVR (approximately 0.6) compared to QDM (approximately 1.1), indicating a better accuracy rate with SVR. RMSE serves as a critical metric, reflecting the average magnitude of prediction errors, while correlation signifies the degree of linear relationship between predictions and observations. However, the homogeneity of the bias correction results using SVR was not comparable to QDM, as reflected in the standard deviation value. The standard deviation of bias correction with QDM closely approximated that of the observations, whereas bias correction with SVR generally resulted in a lower standard deviation. The results indicate that the SVR method produced more consistent results across the dataset, which is vital for ensuring reliable long-term climate projections. Evidence of the homogeneity of the SVR approach was also seen in Figure 1(c), where the bias correction results tended to be centered around zero. In contrast, QDM results were more closely aligned with observations, suggesting that despite SVR's higher statistical performance, QDM may offer more relevant outputs for practical applications. In Figure 1(b), the average T_{mean} per year from all regions of Indonesia, the results from QDM were closer to observations compared to SVR. Although correlation and RMSE showed better results for SVR, the chosen bias correction method for projecting temperatures from 2023 to 2100 was QDM, due to its ability to align more closely with observed data, thus offering greater reliability for future projections.

4.2 Projection of Future Mean Temperature Based on RCP 2.6 and RCP 8.5 Scenarios

T_{mean} projections using the QDM method were applied to global data with the RCP 2.6 and RCP 8.5 emission scenarios from 2023 to 2100. The climate projection results from these two scenarios are presented in Figure 2. The figure showed that the average T_{mean} per year of the two scenarios was relatively similar from 2023 to 2026, but significant differences were seen between 2027 and 2029. This unpredictable phenomenon continued until 2036 when there was a significant difference between the two scenarios from 2037 to 2100. Additionally, in 2024, 2033, and 2036, the annual average T_{mean} of the RCP 2.6 scenario appeared to be higher than RCP 8.5, a scenario with a higher average T_{mean}. Both scenarios indicate that the projected average T_{mean} from 2023 to 2100 tended to increase compared with the historical average from 1950 to 2005. The fluctuations in RCP 2.6 tended to stabilize, while RCP 8.5 showed a significant increase, reaching the average temperature of 30°C daily. Based on the T_{mean} prediction for the RCP 2.6 scenario, Indonesian society was expected to transition to food crop commodities that could withstand high-temperature from 2050 to 2100.

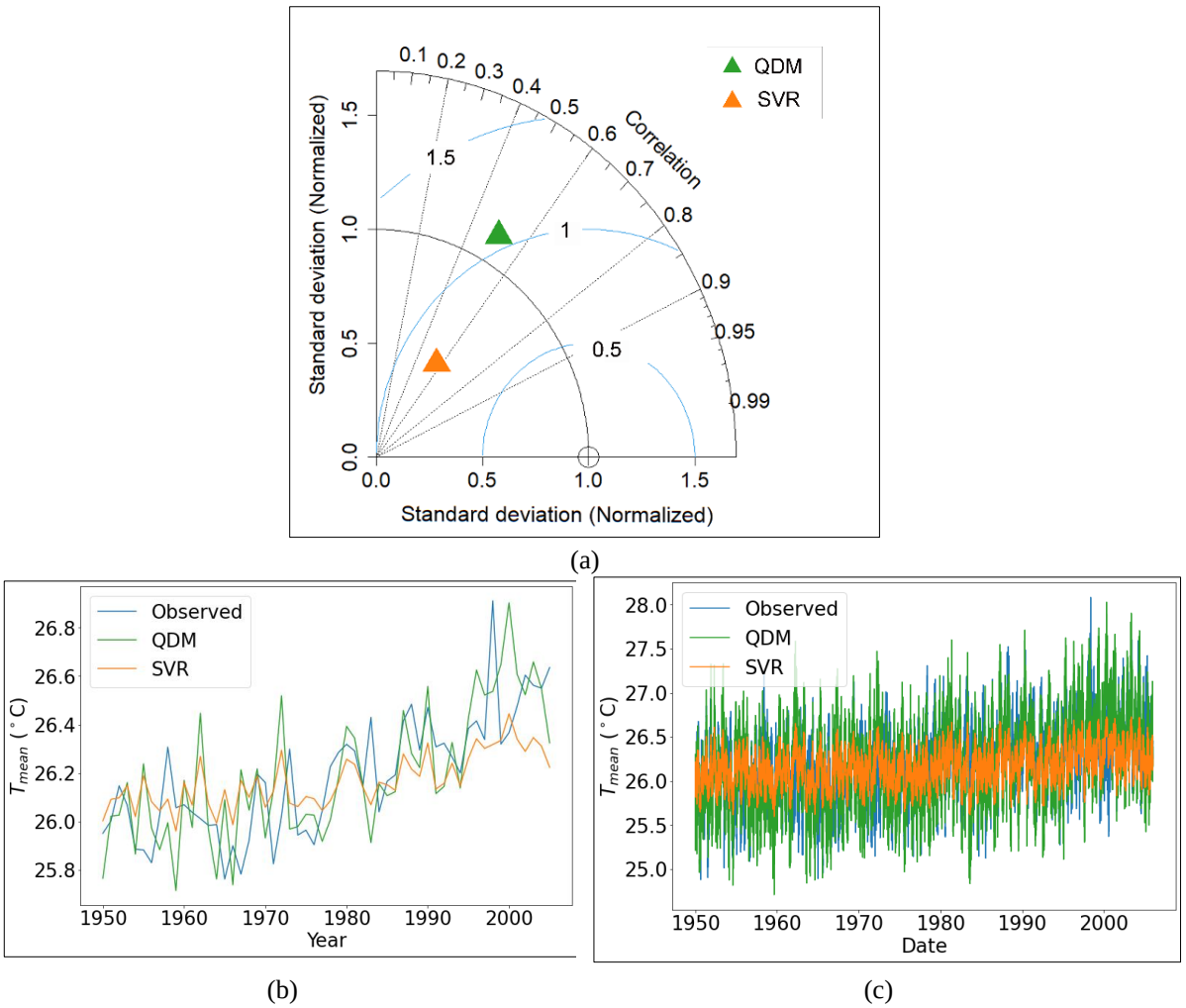

Figure 1 Evaluation method performed using (a) Taylor diagram; (b) Yearly time-series comparison of QDM and SVR of average T_{mean} Yearly; (c) Time Series Plot Comparison Performance of QDM and SVR of average T_{mean} Daily.

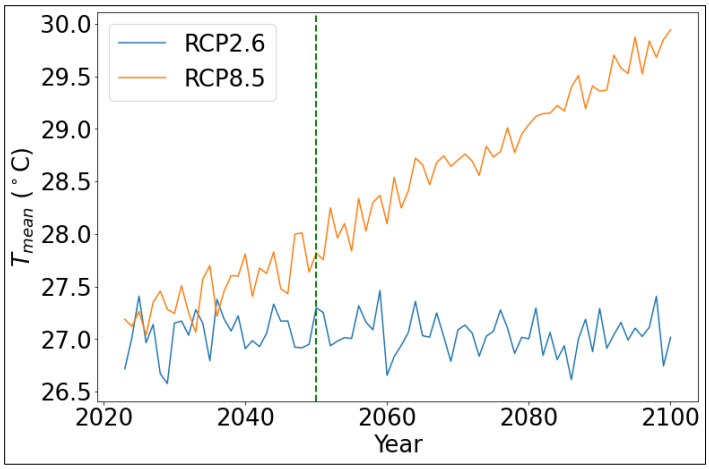

Figure 2 Yearly Average T_{mean} Time Series: Historical Data and Bias Correction Results for RCP 2.6 and RCP 8.5 Scenarios

T_{mean} projections using QDM for the RCP 2.6 and RCP 8.5 scenarios (2023–2100) are shown in Figure 2. The figure showed that the average T_{mean} per year of the two scenarios was relatively similar from 2023 to 2026, but significant differences were seen between 2027 and 2029. This unpredictable phenomenon continued until 2036 before there was a significant difference between the two scenarios from 2037 to 2100. Additionally, in 2024, 2033, and 2036, the annual average T_{mean} of the RCP 2.6 scenario appeared to be higher than RCP 8.5, a scenario with a higher average T_{mean}. Both scenarios showed that the projected average T_{mean} from 2023 to 2100 tended to increase compared with the historical average from 1950 to 2100. RCP 2.6 projections indicate relatively stable temperature fluctuations, whereas RCP 8.5 shows a significant upward trend, with daily average temperatures exceeding 30°C. Based on the T_{mean} prediction for the RCP 2.6 scenario, Indonesian society was expected to transition to food crop commodities that could withstand high-temperature conditions from 2050 to 2100.

Figure 2 shows a notable discrepancy between RCP 2.6 and RCP 8.5. This difference arises from each scenario's fundamentally distinct assumptions regarding future greenhouse gas emissions. RCP 2.6 reflects a low emissions trajectory to limit global warming, leading to more stable climatic conditions that may yield a moderate GSL. Conversely, RCP 8.5 represents a high-emission scenario with minimal mitigation efforts, predicting significant temperature increases and alterations in precipitation patterns that could extend the growing season length in some regions, particularly in areas like Kalimantan and Papua. These regional differences emphasize the necessity of considering both scenarios when planning for agricultural adaptation and resilience in the face of climate change.

Meanwhile, East Nusa Tenggara (NTT), currently the driest and poorest province, was projected to have a relatively lower T_{mean} increase than other provinces in the future, from the RCP 2.6 and RCP 8.5 scenarios. NTT's mainstay agricultural commodities included rice and corn. Even though the T_{mean} increase in NTT was estimated to be lower than in other provinces, factors such as air humidity, rainfall, and soil type remained important factors in optimal growth and production. Fertile and well-drained soil, with a tropical climate and even rainfall, continued to support the development of rice and corn. Therefore, a holistic and scientifically based adaptation strategy must be implemented to maintain food and agricultural security in NTT. Overall, the stippling pattern seen across Indonesia showed a significant change before and after both climate scenarios, RCP 2.6 and RCP 8.5, were implemented.

Examination of the notable T_{mean} differences between the RCP 2.6 (Figure 3(c)) and RCP 8.5 (Figure 3(d)) scenarios revealed a pattern of similarities indicated by stippling. Significant differences were observed in most provinces in Kalimantan, Java, West Nusa Tenggara, and East Nusa Tenggara. On the island of Sumatra, only the Special Region of Aceh and North Sumatra experienced insignificant differences in most areas. Meanwhile, the islands of Sulawesi and Papua showed a similar pattern, where only a few small parts of the region did not show significant differences, such as North Sulawesi, Gorontalo, Mountainous Papua, and Central Papua. The islands of Bangka Belitung, Bali, Maluku, and North Maluku did not show any areas with significant differences in T_{mean} between the two scenarios. However, the difference in average T_{mean} from 2023 to 2050 between the two scenarios tended to be low, with almost all regions of Indonesia showing a difference of less than 0.6 degrees Celsius. However, there was a tendency for the difference to increase from 2051 to 2100, reaching 2.1 degrees Celsius. Based on these results, communities were recommended to plan crop commodity management strategies by considering both scenarios, including which plants were likely to grow and survive in these conditions. This knowledge could become the basis for making more sustainable decisions in dealing with the impacts of climate change.

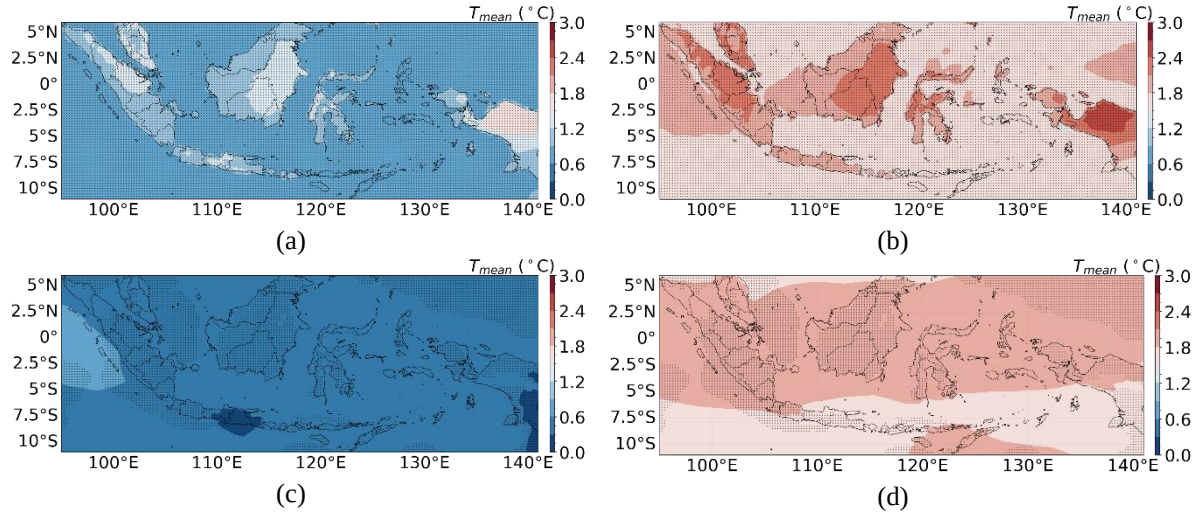

Figure 3 Anomaly of average daily T_{mean} from 2023 to 2073 (a) RCP 2.6 – historical and (b) RCP 8.5 – historical; Differencing of average T_{mean} between RCP 2.6 and RCP 8.5 (c) 2023 to 2050 and (d) 2051 to 2100

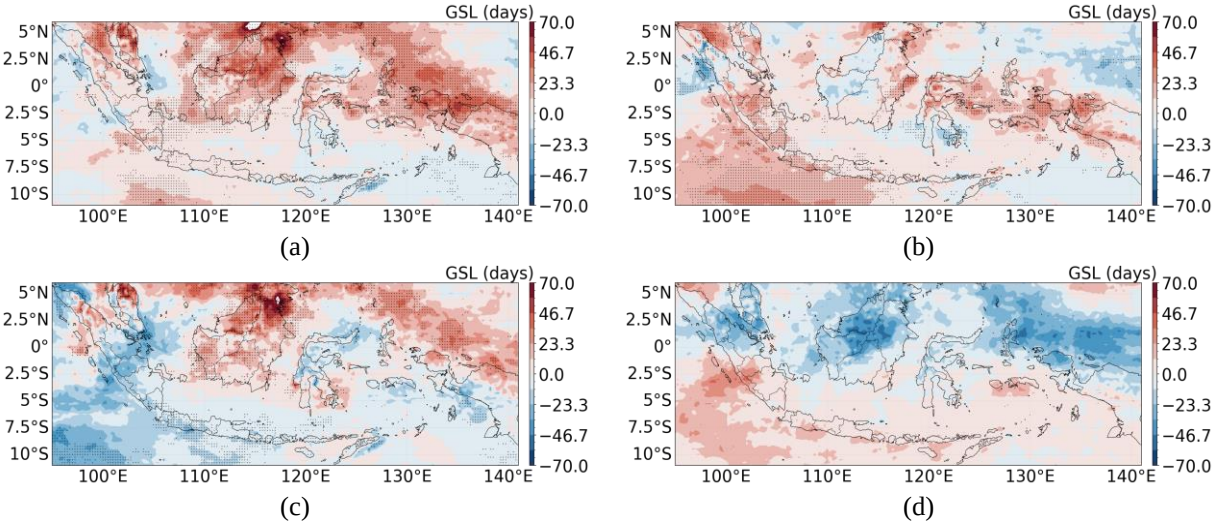

Figure 4 Anomaly of average GSL from 2023 to 2073 (a) RCP 2.6 – historical and (b) RCP 8.5 – historical; Differencing of average GSL between RCP 2.6 and RCP 8.5 (c) 2023 to 2050 and (d) 2051 to 2100

4.3 Projection of Future GSL Based on RCP 2.6 and RCP 8.5 Scenarios

The subsequent analysis examined variations in GSL across Indonesia under two climate change scenarios: RCP 2.6 and RCP 8.5. Figure 4(a) illustrates GSL comparisons between the historical period (1950-2005) and the future projection (2023-2100) for the RCP 2.6 scenario. The findings indicated a notable trend towards an increased GSL across much of Indonesia's terrestrial regions in the future compared to the historical period. Particularly striking increases were observed on the islands of Kalimantan and Papua, notably in North and East Kalimantan, where GSL could extend by up to 58 days. However, there was a decline in GSL in several regions, such as East Nusa Tenggara (NTT), South Sulawesi, Bengkulu, Nias, Siberut, and parts of the southern region of South Papua province. This analysis underscores the importance of considering GSL changes in formulating future climate change adaptation and mitigation policies, particularly regarding planting cycles, harvest schedules, and food resource availability. Steps were needed to monitor and adjust agricultural strategies, identify crops by

GSL changes, and prepare adaptation plans involving farmers and stakeholders.

Meanwhile, a separate analysis compared GSL conditions between historical and future periods under the RCP 8.5 scenario, as depicted in Figure 4(b). The comparison illustrated differences in the projected increase of GSL between RCP 8.5 and RCP 2.6 scenarios, with the most substantial increase anticipated under RCP 8.5 primarily observed in the northern regions of Sumatra. Even though there was an increase in GSL in most of mainland Indonesia in the future, the increase was not as large as in the RCP 2.6 scenario. Significant differences, especially in the Indian Ocean waters, occurred. The findings indicated that under RCP 8.5, the growth in GSL on Kalimantan Island was not substantial compared to RCP 2.6. This conclusion suggested that mitigation policy choices about climate change might influence the impacts of future changes in growing seasons. This analysis provided in-depth insight into the dynamics of GSL change in Indonesia under two different climate change scenarios and the implications for climate change adaptation and mitigation policies. These results highlighted the need for additional research to discover enhanced adaptation strategies and cultivate crop varieties that exhibit greater resilience to climate change, ensuring future food security.

This study examined the average GSL between 2023-2050 and 2051-2100 under the RCP 8.5 and RCP 2.6 scenarios in Indonesia, using the 2.5 degrees South latitude as a demarcation point for comparison. From 2023 to 2050, Figure 4(c) showed that the average GSL in the RCP 8.5 scenario appeared higher than RCP 2.6 in most parts of Indonesia above 2.5 degrees South Latitude. This difference reached almost 70 days. However, in the range from 2051 to 2100, as shown in Figure 4(d), the opposite occurred where the RCP 8.5 scenario showed a lower average GSL compared to RCP 2.6, with a difference of up to 46 days. The conditions diverged in areas of Indonesia situated south of the 2.5 degrees latitude. In this region, the RCP 8.5 scenario appeared higher than RCP 2.6, with an average GSL of 30 days. Significant differences existed between the RCP 8.5 and RCP 2.6 scenarios in most areas of Kalimantan and Java from 2023 to 2050. However, from 2051 to 2100, there were no significant differences in all regions of Indonesia.

5. Discussion

Several bias correction methodologies have been devised across different studies. One research effort evaluated the effectiveness of deep learning models in climate downscaling and bias correction processes. It used daily T_{mean}, T_{min}, and T_{max} data from 20 advanced GCMs sourced from the Coupled Model Intercomparison Project phase 6 (CMIP6). Machine learning models combined univariate and multivariate techniques aimed at effectively correcting for bias and preserving intervariable dependencies among different GCMs regarding observations. Findings showed that machine learning models notably reduced temperature bias compared to conventional methods such as QDM (Wang, & Tian, 2022). However, this study relied solely on residuals in its evaluation. Kuswanto et al., (2022) evaluated three traditional bias correction techniques: Bias Correction Constructed Analogues with Quantile Mapping (BCCAQ), QDM, and Inter-Sectoral Impact Model Intercomparison Project (ISIMIP) for temperature variables (T_{mean}, T_{min}, and T_{max}) in GCM models under RCP 4.5 and G4 scenarios.

The study demonstrated that the QDM method outperformed other approaches in bias correction. Traditional bias correction methods were evaluated based on RMSE, correlation, and standard deviation, whereas machine learning methods primarily assessed performance using error values alone. To address this, Miftahurrohmah et al. (2024) compared the performance of QDM and SVR in T_{mean} bias correction, incorporating RMSE, correlation, and standard deviation in the evaluation process. Their findings revealed that the SVR method was more effective than QDM in reducing bias, particularly in terms of error reduction and correlation improvement. (QDM was better than machine learning methods based on standard deviation because it could better capture pattern variations from observational data. This research demonstrated that the SVR method outperformed QDM regarding bias correction effectiveness, as evidenced by error and correlation metrics. QDM was better than machine learning methods based on standard deviation because it could better capture pattern variations from observational data. This research supported the statement that QDM was better than machine learning and SVR methods in maintaining the standard deviation of data. The comparison of bias correction approaches using SVR and QDM methods revealed insightful findings regarding temperature projection accuracy and homogeneity. Despite SVR showing a higher correlation (0.6) and lower RMSE (approximately 0.6) compared to QDM, QDM demonstrated better homogeneity in bias correction results, aligning closely with

observations. Although SVR yielded homogeneous correction results, its deviation from observations suggested a lack of fit.

Consequently, QDM, despite its slightly inferior correlation and RMSE, was deemed more suitable for projecting T_{mean} from 2023 to 2100. Other research also supported QDM's ability to maintain data homogeneity. However, the data used in this research was rainfall data, which had a high level of heterogeneity compared to temperature. This research compared bias correction without QDM and with QDM, showing that with QDM, the results were better as measured by the RMSE, MAE, and Pearson correlation values. This research did not directly calculate the standard deviation value, but the time series plot results showed that the standard deviation was close to the actual data (Xavier et al., 2022).

By considering data homogeneity, further research could be carried out by bias correction using the SVR method. Bias correction could be started by compiling an algorithm based on the QDM concept and the SVR method. Combining Quantile Delta Mapping (QDM) with Support Vector Regression (SVR) resulted in notably more accurate projections than using each method in isolation. This synergy is particularly beneficial in correcting biases, as QDM effectively captures the distribution of the observed data. At the same time, SVR enhances the model's predictive accuracy through its robust handling of non-linear relationships. The collaborative approach improved the model's performance metrics, such as RMSE and correlation coefficients, and provided a more comprehensive understanding of the underlying climate patterns affecting GSL in Indonesia. Future studies should explore integrating these methods further to optimize bias correction strategies and enhance predictive capabilities in climate modeling.

The research could compare bias correction results using other machine learning methods, whether considering data homogeneity or not. QDM and other quantile-based bias correction methods could also be applied to achieve better results. Previous research had compared bias correction using Quantile Mapping and machine learning methods, especially Long Short-Term Memory (LSTM), for summer daily rainfall (Seo, & Ahn, 2023). The results showed that Quantile Mapping (QM) was superior to LSTM in bias correction, with correlation, RMSE, and standard deviation metrics showing better performance for QM. The QM method explained that the standard deviation was almost perfect, and the performance evaluation of each method was carried out every group of months, consisting of daily data. The QM method has been proven to maintain the stability of data homogeneity (Cannon et al., 2015). Deep learning methods and their customization could also be considered in this research. Deep learning customization had been tested for precipitation data's downscaling and bias correction process. The test results showed that customized deep learning was better than regular deep learning and statistical methods for downscaling and bias correction. However, this evaluation was based only on error rates such as RMSE and MAE (Wang et al., 2023). Evaluation to measure the homogeneity of data also needed to be implemented. Furthermore, investigations into the scalability and transferability of bias correction methods across diverse geographical regions and climate scenarios were warranted. Understanding how these methods perform under varying environmental conditions and emission scenarios would be crucial for robust climate impact assessments and adaptation planning on a global scale. Future research could include a comparison with the Random Forest algorithm to evaluate predictive performance further.

Applying the QDM method to project T_{mean} under RCP 2.6 and RCP 8.5 scenarios unveiled significant temporal differences, particularly beyond 2026. While both scenarios anticipated rising T_{mean} compared to historical averages, RCP 8.5 exhibited more pronounced fluctuations and an eventual surge, surpassing 30°C. This escalation prompted recommendations for transitioning to heat-resistant food crop commodities by 2050-2100. Provincial T_{mean} projections under RCP 2.6 and RCP 8.5 scenarios underscored diverse regional impacts. Papua experienced substantial temperature anomalies, urging adaptation strategies for agriculture.

Conversely, East Nusa Tenggara foresaw comparatively minor T_{mean} increases, emphasizing the importance of holistic adaptation plans considering local conditions. Analysis of T_{mean} differences between RCP 2.6 and RCP 8.5 scenarios revealed nuanced regional disparities. Kalimantan, Java, and certain islands exhibited significant variations, necessitating meticulous crop management strategies tailored to scenario-specific conditions. Further analysis of GSL under RCP 2.6 and RCP 8.5 scenarios elucidated contrasting temporal trends. While RCP 2.6 implied substantial GSL increases, RCP 8.5 forecasted a more modest rise, emphasizing the pivotal role of mitigation policies in shaping future growing seasons. Overall, this study elucidated the multifaceted impacts of climate change on T_{mean}

patterns and GSL in Indonesia. The findings underscored the urgency of implementing adaptive measures and fostering resilient agricultural practices to mitigate the adverse effects of climate change and ensure food security in the future. Future research endeavors should prioritize identifying effective adaptation strategies and developing climate-resilient crop varieties to safeguard Indonesia's agricultural sustainability amidst evolving climatic conditions.

In our future work, we anticipate leveraging AI technologies to enhance the accuracy and efficiency of climate modeling and bias correction methodologies. Specifically, we aim to explore the integration of advanced machine learning algorithms, such as deep learning and ensemble methods, to capture complex relationships within climate data better. These AI approaches will facilitate improved predictive capabilities, allowing for more precise projections of temperature and GSL trends. Furthermore, we hope to develop user-friendly tools that enable practitioners to apply these AI methods easily in their research, thereby fostering broader adoption and collaboration in climate science. By harnessing the power of AI, we envision significant advancements in our understanding of climate dynamics and more effective strategies for adaptation of climate change.

6. Conclusion

The SVR method outperformed QDM in terms of RMSE and correlation. Although the correlation between SVR and QDM was insignificant (0.6 and 0.5, respectively), SVR exhibited a clearer advantage in RMSE, with a value of 0.6 compared to 1.1 for QDM. However, in terms of homogeneity or deviation, QDM was superior, as its results were closer to the homogeneity of observations. Based on these findings, the preferred method for T_{mean} projection was QDM due to its ability to maintain data homogeneity. Projections of future T_{mean} and GSL under RCP 2.6 and RCP 8.5 scenarios indicated a significant increase in T_{mean} after 2026, with RCP 8.5 predicting spikes in T_{mean} exceeding 30°C. The results underscore the need for using heat-resistant food commodities by 2050-2100. Meanwhile, GSL under RCP 2.6 increased more than under RCP 8.5, highlighting the importance of mitigation policies.

This study demonstrated the urgency of implementing adaptive and resilient agricultural practices to address climate change and maintain food security in Indonesia. Future research should focus on effective adaptation strategies and developing climate-resilient crop varieties. It is anticipated that bias correction can utilize SVR or other machine learning methods, considering data consistency with observations. The combination of QDM and SVR could also be explored for bias correction. Other quantile-based methods, including their combination with machine learning techniques, may be employed to identify the best bias correction approach. Further research is also needed on the scalability and transferability of bias correction methods across different geographical regions and climate scenarios. Understanding the performance of these methods under various environmental conditions and emission scenarios is crucial for accurate climate impact assessments and effective adaptation planning globally.

Future research could involve applying this combined approach to historical climate data to validate further our methodology and the cooperation between the SVR and QDM methods. By analyzing past datasets, we aim to assess the accuracy and effectiveness of our criteria and techniques in replicating observed temperature and GSL trends. This validation would reinforce our methods' reliability and provide insights into their applicability in various climatic conditions. Additionally, it would allow for a comprehensive evaluation of how well our model can capture historical patterns, thereby strengthening the foundation for its application in future climate projections.

7. Acknowledgements

Acknowledgments are given to the The Ministry of Education, Culture, Research, and Technology for providing funding to researchers enabling the smooth execution of this research. The acknowledgments are also given to Lembaga Penelitian dan Pengabdian Masyarakat Universitas Internasional Semen Indonesia (LPPM UISI) who has helped in the administrative activities of this research.

8. References

Amien, L. I., & Runtunuwu, E. (2009). Agrometeorological Data And Rainfall Forecasting For Crop Simulation. *Jurnal Sumber Daya Lahan, 3*(2), 61–72. https://doi.org/10.2018/jsdl.v3i02.185

Arslantaş, E. E., & Yeşilırmak, E. (2020). Changes in the climatic growing season in Western Anatolia, Turkey. *Meteorological Applications, 27*(2), Article e1897. https://doi.org/10.1002/met.1897

Largeau, A., Wongprathed, J., Wongwailikhit, K., Dietrich, N., Soottitantawat, A., Methaapanon,

R., Beghin, R., Frayssignes, J., & Hébrard, G. (2024). *An inspiring way to reach carbon neutrality: Aqueous carbonation of coal and biomass ashes.* Paper presented at the International Congress of Chemical and Process Engineering, Prague, Czech Republic. https://hal.archives-ouvertes.fr/hal-04782905

Barnard, D. M., Knowles, J. F., Barnard, H. R., Goulden, M. L., Hu, J., Litvak, M. E., & Molotch, N. P. (2018). Reevaluating growing season length controls on net ecosystem production in evergreen conifer forests. *Scientific Reports*, *8*(1), Article 36065. https://doi.org/10.1038/s41598-018-36065-0

Brown, M. E., Antle, J. M., Backlund, P., Carr, E. R., Easterling, W. E., Walsh, M. K., … & Tebaldi, C. (2015). *Climate Change, Global Food Security, and the U.S. Food System*. Retrieved from https://ageconsearch.umn.edu/record/337546/?v=pdf

Calinger, K., & Curtis, P. (2023). A century of climate warming results in growing season extension: Delayed autumn leaf phenology in north-central North America. *PLOS ONE, 18*(3), Article e0282391. https://doi.org/10.1371/journal.pone.0282391

Cannon, A. J., Sobie, S. R., & Murdock, T. Q. (2015). Bias correction of GCM precipitation by quantile mapping: How well do methods preserve changes in quantiles and extremes?. *Journal of Climate*, *28*(17), 6938–6959. https://doi.org/10.1175/JCLI-D-14-00754.1

Cech, R., Leisch, F., & Zaller, J. G. (2022). Pesticide use and associated greenhouse gas emissions in sugar beet, apples, and viticulture in Austria from 2000 to 2019. *Agriculture, 12*(6), Article 879. https://doi.org/10.3390/agriculture12060879

Chancellor, W., Hughes, N., Zhao, S., Soh, W. Y., Valle, H., & Boult, C. (2021). Controlling for the effects of climate on total factor productivity: A case study of Australian farms. *Food Policy*, *102*, Article 102091. https://doi.org/10.1016/j.foodpol.2021.102091

Chen, W., Zorn, P., White, L., Olthof, I., Zhang, Y., Fraser, R., & Leblanc, S. (2016). Decoupling between Plant Productivity and Growing Season Length under a Warming Climate in Canada's Arctic. *American Journal of Climate Change*, *5*(3), 334–359. https://doi.org/10.4236/ajcc.2016.53026

Cho, D., Yoo, C., Im, J., & Cha, D. H. (2020). Comparative assessment of various machine learning-based bias correction methods for numerical weather prediction model forecasts of extreme air temperatures in urban areas. *Earth and Space Science, 7*(4), Article e2019EA000740. https://doi.org/10.1029/2019EA000740

Fauzi, F., Kuswanto, H., & Atok, R. M. (2020). Bias correction and statistical downscaling of earth system models using quantile delta mapping (QDM) and bias correction constructed analogues with quantile mapping reordering (BCCAQ). *Journal of Physics: Conference Series*, *1538*(1), 1–9. https://doi.org/10.1088/1742-6596/1538/1/012050

Fernie, E., Tan, D. K. Y., Liu, S. Y., Ullah, N., & Khoddami, A. (2022). Post-Anthesis Heat Influences Grain Yield, Physical and Nutritional Quality in Wheat: A Review. *Agriculture (Switzerland), 12*(6), 1–24. https://doi.org/10.3390/agriculture12060886

Gouveia, C. M., Justino, F., Gurjao, C., Zita, L., & Alonso, C. (2023). Revisiting Climate-Related Agricultural Losses across South America and Their Future Perspectives. *Atmosphere*, *14*(8), 1–20. https://doi.org/10.3390/atmos14081303

Hinze, J., Albrecht, A., & Michiels, H. G. (2023). Climate-Adapted Potential Vegetation—A European Multiclass Model Estimating the Future Potential of Natural Vegetation. *Forests*, *14*(2), 1–19. https://doi.org/10.3390/f14020239

Huang, L., Fang, X., Zhang, T., Wang, H., Cui, L., & Liu, L. (2023). Evaluation of surface temperature and pressure derived from MERRA-2 and ERA5 reanalysis datasets and their applications in hourly GNSS precipitable water vapor retrieval over China. *Geodesy and Geodynamics*, *14*(2), 111–120. https://doi.org/10.1016/j.geog.2022.08.006

Hudson, A. R., Smith, W. K., Moore, D. J. P., & Trouet, V. (2022). Length of growing season is modulated by Northern Hemisphere jet stream variability. *International Journal of Climatology*, *42*(11), 5644–5660. https://doi.org/10.1002/joc.7553

Hunter, R. D., & Meentemeyer, R. K. (2005). Climatologically aided mapping of daily precipitation and temperature. *Journal of Applied Meteorology*, *44*(10), 1501–1510. https://doi.org/10.1175/JAM2295.1

Intergovernmental Panel on Climate Change (IPCC). (2015). Climate change 2014: Synthesis report.

Contribution of Working Groups I, II and III to the Fifth Assessment Report of the Intergovernmental Panel on Climate Change (R. K. Pachauri & L. A. Meyer, Eds.). In *Managing the Risks of Extreme Events and Disasters to Advance Climate Change Adaptation: Special Report of the Intergovernmental Panel on Climate Change*. IPCC. https://doi.org/10.1017/CBO9781139177245.003

Jubb, I., Canadell, P., & Dix, M. (2013). *Representative concentration pathways*. Australian Government, Department of the Environment. https://www.environment.gov.au/

Khairulbahri, M. . (2022). Understanding the Impacts of Climate Change on Rice Production: A Qualitative Perspective. *Science & Technology Asia*, *27*(1), 169–179. https://ph02.tci-thaijo.org/index.php/SciTechAsia/article/view/242411

Kumar, V., Kumari, A., Price, A. J., Bana, R. S., Singh, V., & Bamboriya, S. D. (2023). Impact of futuristic climate variables on weed biology and herbicidal efficacy: A review. *Agronomy*, *13*(2), Article 559. https://doi.org/10.3390/agronomy13020559

Kumari, A., Lakshmi, G. A., Krishna, G. K., Patni, B., Prakash, S., Bhattacharyya, M., & Verma, K. K. (2022). Climate change and its impact on crops: A comprehensive investigation for sustainable agriculture. *Agronomy*, *12*(12), Article 3008. https://doi.org/10.3390/agronomy12123008

Kuswanto, H., Kravitz, B., Miftahurrohmah, B., Fauzi, F., Sopahaluwaken, A., & Moore, J. (2022). Impact of solar geoengineering on temperatures over the Indonesian Maritime Continent. *International Journal of Climatology*, *42*(5), 2795–2814. https://doi.org/10.1002/joc.7391

Liu, E., Zhou, G., He, Q., Wu, B., Zhou, H., & Gu, W. (2022). Climatic mechanism of delaying the start and advancing the end of the growing season of *Stipa krylovii* in a semi-arid region from 1985 to 2018. *Agronomy*, *12*(8), Article 1906. https://doi.org/10.3390/agronomy12081906

Miftahurrohmah, B., Kuswanto, H., Pambudi, D. S., Fauzi, F., & Atmaja, F. (2024). Assessment Assessment of of the the Support Support Vector Regression Regression and Random Random Forest Algorithms in the Bias Bias Correction Process on Temperatures Algorithms. *Procedia Computer Science*, *234*, 637–644. https://doi.org/10.1016/j.procs.2024.03.049

Montero-Martínez, M. J., & Andrade-Velázquez, M. (2022). Effects of urbanization on extreme climate indices in the Valley of Mexico Basin. *Atmosphere*, *13*(5), Article 785. https://doi.org/10.3390/atmos13050785

National Climate Change Adaptation Research Facility. (2017). *How to use climate change scenarios*. Retrieved from https://coastadapt.com.au/how-to-pages/how-to-use-climate-change-scenarios-to-evaluate-risk-plan-and-make-decisions

Ngongondo, C. O. S. M. O., Tallaksen, L. M., & Xu, C. Y. (2014). Growing season length and rainfall extremes analysis in Malawi. In *Hydrology in a changing world: Environmental and human dimensions* (pp. 361–365). International Association of Hydrological Sciences (IAHS) Publications, 363, 361-365.

Park, T., Ganguly, S., Tømmervik, H., Euskirchen, E. S., Høgda, K. A., Karlsen, S. R., & Myneni, R. B. (2016). Changes in growing season duration and productivity of northern vegetation inferred from long-term remote sensing data. *Environmental Research Letters*, *11*(8), Article 084001. https://doi.org/10.1088/1748-9326/11/8/084001

Petchchedchoo, P., Petcharaks, N., Piratrakul, P., & Wongmuek, K. (2024). Analysis of the carbon footprint of academic gowns: a case study of thai university. *Journal of Current Science and Technology*,*14*(2), Article 46. https://doi.org/10.59796/jcst.V14N2.2024.46

Potisomporn, P., Adcock, T. A. A., & Vogel, C. R. (2023). Evaluating ERA5 reanalysis predictions of low wind speed events around the UK. *Energy Reports*, *10*, 4781–4790. https://doi.org/10.1016/j.egyr.2023.11.035

Qi, Y., Zhang, Q., Hu, S., Wang, R., Wang, H., Zhang, K., & Yang, Y. (2022). Effects of high temperature and drought stresses on growth and yield of summer maize during grain filling in North China. *Agriculture*, *12*(11), Article 1948. https://doi.org/10.3390/agriculture12111948

Rajulapati, C. R., & Papalexiou, S. M. (2023). Precipitation bias correction: A novel semi-

parametric quantile mapping method. *Earth and Space Science*, *10*(4), Article e2023EA002823. https://doi.org/10.1029/2023EA002823

Seo, G.-Y., & Ahn, J.-B. (2023). Comparison of bias correction methods for summertime daily rainfall in South Korea using quantile mapping and machine learning models. *Atmosphere*, *14*(7), Article 1057. https://doi.org/10.3390/atmos14071057

Tan, M. L., Armanuos, A. M., Ahmadianfar, I., Demir, V., Heddam, S., Al-Areeq, A. M., & Yaseen, Z. M. (2023). Evaluation of NASA POWER and ERA5-Land for estimating tropical precipitation and temperature extremes. *Journal of Hydrology*, *624*, Article 129940. https://doi.org/10.1016/j.jhydrol.2023.129940

Tan, Y., Guzman, S. M., Dong, Z., & Tan, L. (2020). Selection of effective GCM bias correction methods and evaluation of hydrological response under future climate scenarios. *Climate*, *8*(10), Article 108. https://doi.org/10.3390/cli8100108

Ukaew, S., Tungtakanpoung, D., & Chongsithiphol, S. (2020). An assessment of life cycle greenhouse gas emissions for day spa services in Eastern Thailand: A case study in Chonburi, Rayong, and Trad provinces. *Naresuan University Journal: Science and Technology*, *28*(1), Article 1. https://doi.org/10.14456/nujst.2020.1

Villa-Falfán, C., Valdés-Rodríguez, O. A., Vázquez-Aguirre, J. L., & Salas-Martínez, F. (2023). Climate indices and their impact on maize yield in Veracruz, Mexico. *Atmosphere*, *14*(5), Article 778. https://doi.org/10.3390/atmos14050778

Wang, F., & Tian, D. (2022). On deep learning-based bias correction and downscaling of multiple climate models simulations. *Climate Dynamics*, *59*(11–12), 3451–3468. https://doi.org/10.1007/s00382-022-06277-2

Wang, F., Tian, D., & Carroll, M. (2023). Customized deep learning for precipitation bias correction and downscaling. *Geoscientific Model Development*, *16*(2), 535–556. https://doi.org/10.5194/gmd-16-535-2023

Wang, J. W., Li, M., Zhang, G. Y., Zhang, H. R., & Yu, C. Q. (2020). Growing season precipitation rather than growing season length predominates maximum normalized difference vegetation index in alpine grasslands on the Tibetan Plateau. *Sustainability*, *12*(3), Article 968. https://doi.org/10.3390/su12030968

Xavier, A. C. F., Martins, L. L., Rudke, A. P., de Morais, M. V. B., Martins, J. A., & Blain, G. C. (2022). Evaluation of Quantile Delta Mapping as a bias-correction method in maximum rainfall dataset from downscaled models in São Paulo state (Brazil). *International Journal of Climatology*, *42*(1), 175–190. https://doi.org/10.1002/joc.7238

Yilmaz, M. (2023). Accuracy assessment of temperature trends from ERA5 and ERA5-Land. *The Science of The Total Environment*, *856*(2), Article 159182. https://doi.org/10.1016/j.scitotenv.2022.159182

Zare, M., Azam, S., Sauchyn, D., & Basu, S. (2023). Assessment of meteorological and agricultural drought indices under climate change scenarios in the South Saskatchewan River Basin, Canada. *Sustainability*, *15*(7), Article 5907. https://doi.org/10.3390/su15075907

Zhou, Y. (2020). Relative contribution of growing season length and amplitude to long-term trend and interannual variability of vegetation productivity over northeast China. *Forests*, *11*(1), Article 112. https://doi.org/10.3390/f11010112